Analytical Biochemistry 398 (2010) 191–197

Contents lists available at ScienceDirect

Analytical Biochemistry

journal homepage: www.elsevier.com/locate/yabio

Hydroxyapatite nanoarray-based cyanide biosensor

Suiping Wang [a,b], Yong Lei [a], Yun Zhang [a], Jian Tang [a], Guoli Shen [a,*], Ruqin Yu [a]

[a] State Key Laboratory for Chemo/Biosensing and Chemometrics, College of Chemistry and Chemical Engineering, Hunan University, Changsha 410082, People's Republic of China
[b] Food Science and Engineering College, Jiangxi Agriculture University, Nanchang 330045, People's Republic of China

ARTICLE INFO

Article history:
Received 3 July 2009
Received in revised form 31 October 2009
Accepted 19 November 2009
Available online 26 November 2009

Keywords:
Hydroxyapatite nanowires array
Cyanide
Inhibition biosensor
Electrochemical

ABSTRACT

Here we report a simple, biomolecular-friendly protocol for the fabrication of a hydroxyapatite nanowires array (HANWA) biosensor of spatial positioning, large surface area, and abundant adsorbing sites and its application to cyanide sensing. The fabrication of HANWA is performed by template-assisted electrodeposition. The well-aligned hydroxyapatite nanoarray is composed of vertical nanowires with a diameter of approximately 200 nm and an average length of 1 μm. The electrochemical biosensor for the determination of cyanide through its inhibitory effect on horseradish peroxidase (HRP) encapsulated by chitosan (CHIT) on the platform of HANWA is demonstrated. The current organic–inorganic hybrid nanostructure provides excellent enzyme–substrate contact with enzyme activity well maintained. The densely distributed HANWA with large surface area and abundant adsorbing sites can provide a favorable electrochemical interface for the construction of electrochemical biosensor. A sensitive detection limit of 0.6 ng ml^{-1} was obtained for cyanide. The proposed CHIT–HRP/HANWA biosensor has the advantages of spatial resolution, high sensitivity, rapid regeneration, and fast response associated with individual nanowires. It broadens the possible applications of chemosensors and biosensors, and it offers an alternative method for toxic substance determination. The new device holds great promise for environmental and food industrial monitoring of toxins.

Nanostructure materials are very attractive due to their unique chemical and physical properties and have found potential applications in nanoelectronic devices, catalysts, and drug delivery/release. During the past few years, the exploration of synthetic techniques for the fabrication of nanostructure materials with controllable morphologies has emerged as a fast-growing subfield of nanotechnology research. Particular attention has been directed toward one-dimensional nanostructures, such as nanotubes and nanowires [1–3], whose properties and effects (e.g., high aspect ratio, higher storage and velocity of information transmission, blue shift of absorption edge of nanoparticles, quantization of conductance, enhanced mechanical properties) lead to functionalized material arrays and research on transport phenomena at nanometric scale. The application of nanoarrays for biosensors is currently an increasing trend; the ingeniously designed nanoarray biosensors bring greatly improved performance [4,5].

Hydroxyapatite [HA,[1] $Ca_5(PO_4)_3(OH)$], a bioceramic analogous to the mineral component of bone with great biocompatibility and particular multiadsorbing sites, has been applied extensively in adsorbents and protein separation [6–8]. Due to the excellent biocompatibility and adsorbability, HA has begun to be used in biosensors during recent years. Up to now, HA-based (bio)sensors are very few in number [9–11]. HA powders are conventionally synthesized by various methods, including solid-state reaction, precipitation and hydrolysis of calcium phosphates, sol–gel, and emulsion techniques [12]. The size- and shape-dependent nanostructured HA would ultimately exert the biocompatibility and bioactivity for the design of nanodevices, relating to the advantages of multiadsorbing sites, large surface area, multifunction ability, and high biocompatibility. The polysaccharide biopolymer chitosan (CHIT), due to the presence of reactive amino and hydroxyl function groups, displays excellent film-forming ability, high water permeability, good adhesion, and susceptibility to chemical modifications [13,14]. The combination of nanostructured materials and biomaterials for biosensing is encouraging.

Cyanide is an extremely poisonous compound that can bind to the iron in cytochrome *c* oxidase, interferes with electron transport, and results in hypoxia. It is commonly used in industries such as precious metal mining, metal plating shops, steel mills, and plastic and fertilizer factories. The various industries worldwide produce as much as 1.4 million tons of toxic cyanide per year, which is a dangerous potential contaminant to drinking water, food, and the environment. Some food plants can also release

* Corresponding author. Fax: +86 731 8821355.
E-mail address: glshen@hnu.cn (G. Shen).

[1] *Abbreviations used:* HA, hydroxyapatite; CHIT, chitosan; HANWA, hydroxyapatite nanowires array; HRP, horseradish peroxidase; PC, polycarbonate; PBS, phosphate-buffered saline; SEM, scanning electron microscopy; GCE, glassy carbon electrode; SCE, saturated calomel electrode; CV, cyclic voltammogram; RSD, relative standard deviation.

0003-2697/$ - see front matter © 2010 Elsevier Inc. All rights reserved.
doi:10.1016/j.ab.2009.11.029

cyanide because of their content of cyanogenic glycosides. Cyanogenesis is known to occur in the plant genera *Prunus, Sambucus, Linum, Carica, Phaseolus,* and *Manihot*. Current cyanide detection methods include titrimetric, calorimetric, potentiometric, and spectrophotometric determinations as well as flow injection, ion chromatography, and headspace gas chromatography analyses [15–20]. In spite of the advantages, these techniques require expensive instrumentation and highly trained personnel, which are usually time-consuming and not easily adapted for rapid analysis. Considering the acute toxicity of cyanide and its potential contamination in the environment and food, there is a pressing need for fast accurate detection of cyanide at regulated concentrations. Biosensors could be a reliable and promising alternative to classical methods because of their simplicity, high sensitivity, rapid analysis, and good selectivity. The demand for reliable and inexpensive methods for food quality assessment is increasing, and biosensors are ideal candidates for improving food diagnostics [21].

Biosensors based on the principle of enzyme inhibition have been applied for a wide range of significant analytes such as pesticides, heavy metal ions, and other toxic compounds [22,23]. The modulated biocatalytic activity accrued from the enzyme–inhibitor interaction is commonly detected from the decreased electrochemical response of the corresponding substrate. Enzyme inhibitor detectors can be very sensitive to toxic agents, with an extremely low detection limit that depends on the binding affinity of the enzyme–inhibitor system.

Here we report a simple, biomolecular-friendly protocol for the fabrication of a cyanide inhibition biosensor based on hydroxyapatite nanowires array (HANWA) with the sensing element of horseradish peroxidase (HRP). The fabrication of HANWA is performed by template-assisted electrodeposition. The biocompatibility, permeability, and electron transfer efficiency within the immobilization matrix are the main factors consequently affecting the performance of the biosensor. The combination of HANWA and CHIT provides an excellent sensing interface for biological sensing element immobilization and electrochemical transduction with regard to the loading density, orientation, and bioactivity of the bioreceptor that has contributed to the high sensitivity of the cyanide biosensor.

Materials and methods

Apparatus and reagents

Track-etched porous polycarbonate (PC, 0.2 μm) membrane was provided by Whatman. A thin film of gold was sputtered onto one side of the PC membrane for conductivity before use. HRP (250 U/mg) was purchased from Kaiyang (Shanghai, China). $Ca(NO_3)_2$, $NH_4H_2PO_4$, and any other reagents all were of analytical grade and purchased from Sinopharm Chemical Reagent (Shanghai, China). The standard stock solution of KCN (100 mg L^{-1}), obtained from the Hunan Provincial Center of Disease Prevention and Control, was prepared by dissolving 0.25 g of potassium cyanide in ultrapure water to 1 L and calibrated with silver nitrate. The concentration of cyanide was calculated as the mass concentration of CN^-. (Because cyanide is a dangerous toxic compound, precautions must be taken to prevent any accidental release. The solution should be kept away from acidity to avoid HCN liberation and vaporization. Experiments should be performed in a well-aerated room.) The supporting electrolyte was 10 mM sodium phosphate-buffered saline (PBS, pH 7.0) containing 0.1 M KCl unless otherwise stated. Ultrapure water was used throughout with a resistance of 18.2 MΩ cm.

Scanning electron microscopy (SEM) analysis was performed using a JSM-5600LV microscope (Jeol, Tokyo, Japan). Electrochemical measurements were carried out on CHI 760B electrochemical workstation (Shanghai, China). A three-electrode cell (5 ml) was used with a modified glassy carbon electrode (GCE) as the working electrode, a saturated calomel electrode (SCE) as the reference electrode, and a platinum foil electrode as the counter electrode. All potentials were measured and reported versus the SCE, and all experiments were carried out at room temperature.

Fabrication of the HA nanoarray

GCEs (4 mm diameter) were polished with emery paper and alumina slurry consecutively, cleaned under bath sonication with water and ethanol alternatively, and finally rinsed thoroughly with distilled water. PC template was carefully attached onto the GCE surface and adhered by silver paint. HANWA was synthesized directly on GCE by means of cathode electrodeposition with the aid of PC membrane. The electrodeposition condition was referenced from previous literature with slight modification [24]. Typical procedures to fabricate HANWA that were eventually adopted in this work are as follows: constant cathode current electrodeposition was performed under a current density of 0.005 mA mm^{-2} for 5 min in solutions containing 42 mM $Ca(NO_3)_2$ and 25 mM $NH_4H_2PO_4$, and then the PC template was released by dissolving in chloroform.

Construction of the enzyme electrode

CHIT solution (0.5 wt%) was prepared by dissolving 0.025 g of CHIT flakes in 5 ml of acetic acid (1.0%) and was stirred at room temperature until complete dissolution. Equal volumes of 10 mg ml^{-1} HRP and 0.5 wt% CHIT were mixed sufficiently, and 8 μl of the mixture was cast onto the surface of HANWA modified GCE and left to air dry. The fabricated biosensor was stored at 4 °C when not in use. The modified electrode is denoted as CHIT–HRP/HANWA/GCE; other denotations are made in a similar manner.

Electrochemical measurements

All electrochemical measurements were performed in a conventional three-electrode system with a modified GCE as the working electrode, an SCE as the reference electrode, and a platinum foil electrode as the counter electrode. Cyclic voltammetry was carried out in 10 mM PBS containing 0.1 M KCl. Alternating current impedance behavior was obtained in 10 mM PBS (pH 7.4) containing 0.1 M KCl and 5 mM $K_3[Fe(CN)_6]/K_4[Fe(CN)_6]$ with a frequency range from 1 to 100,000. Chronoamperometry was performed in 5 ml of PBS by applying a working potential of −0.1 V under constant stirring.

Characterizations of cyanide biosensor's inhibition performance

Cyclic voltammetric measurements were carried out in the potential range from −0.4 to 0.6 V at a scan rate of 100 mV s^{-1} in PBS before and after the addition of H_2O_2 or cyanide under non-stirring conditions. Chronoamperometric measurements were carried out in 5 ml of PBS with H_2O_2 added. When the catalytic transient currents decayed to a steady-state value, 5 μl of specific concentration of cyanide was quickly added. The steady-state catalytic current was recorded as I_0 according to the initial baseline current. The current response in the case of the specific concentration of cyanide due to the inhibition of the enzyme activity was recorded as I_1. The inhibitory signal was correlated to the concentration of cyanide. Typical calibration curves were based on the percentage of inhibition (I) as a function of the concentration of cyanide. The per-

centage of inhibition was calculated using the following relationship [22]: $I(\%) = [(I_0 - I_1)/I_0] \times 100$, where I_0 and I_1 are the current signal before and after cyanide introduction in the presence of the enzyme substrate (H_2O_2) and I_1 is expected to be smaller than I_0 for the inhibited enzyme activity by cyanide.

Determination of cyanide in real sample

Tap water was used directly for recovery studies without pretreatment. The sample of river water, distilled wine, and edible cassava starch was distilled under acidic conditions using alkali solution for the absorption of hydride cyanide, pretreated by the standard methods of GB/T 5750-2001, GB/T 5009, 48-2003 and NY/T 875-2004, and then was analyzed by the proposed biosensor and the classical calorimetric method. The quantitative principle of the calorimetric method is that the oxidized cyanide of the CNCl complex using chloroamine-T can form a blue-colored solution by the addition of a pyridine–pyrazole or pyridine–barbituric acid reagent, which can be determined by the adsorption intensity at 638 nm.

Results and discussion

Morphology of HANWA

The surface topology of the modified GCE was characterized by SEM. Fig. 1 shows the SEM images of the high-density and well-aligned nanowires of HANWA. The vertical nanowires of HANWA are highly regular and ordered, with a diameter of approximately 200 nm and an average length of 1 μm. The diameter of the nanowires is in good agreement with that of the PC template's nanopores. With respect to the high surface area, great biocompatibility, and particular multiadsorbing sites, HANWA can be applied to fabricate the biosensor effectively. It can be seen that the space between two neighboring nanowires is significantly larger than their diameter; so that each nanowire can be worked as an individual nanoelectrode when immobilized with enzyme [25]. According to the SEM images, the array density of the nanowires is estimated to be 5×10^8 cm^{-2}.

Electrochemical characteristics of sensing surface

Electrochemical impedance spectroscopy is one of the most powerful and sensitive techniques for investigating the features of surface-modified electrodes. The impedance spectrum includes

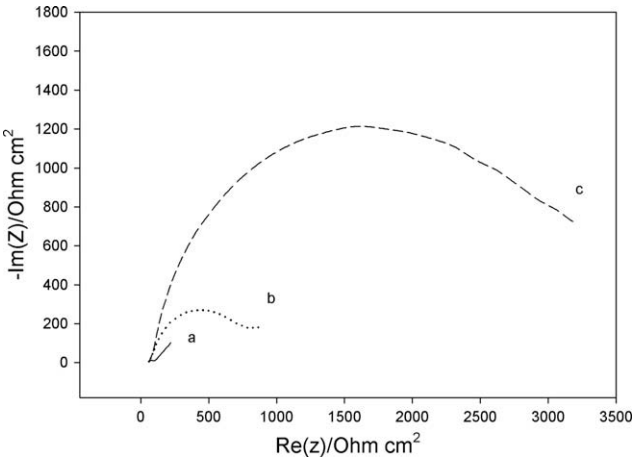

Fig. 2. Nyquist diagrams of electrochemical impedance for the different modification stages: (a) bare GCE; (b) GCE modified with HANWA; (c) curve b immobilized with CHIT–HRP. The frequency range was from 1 Hz to 100 kHz, and the amplitude of the alternating voltage was 5 mV. All measurements were performed in 10 mM PBS (pH 7.0) containing 0.1 M KCl and 5 mM $K_3[Fe(CN)_6]/K_4[Fe(CN)_6]$.

a semicircle portion at higher frequencies corresponding to the electron transfer-limiting process and a linear part at the low frequencies resulting from the diffusion-limiting step of the electrochemical process. The diameter corresponding to the electron transfer resistance (R_{et}) can be used to describe the interface properties of the electrode. Fig. 2 shows Nyquist diagrams of electrochemical impedance for the different modification stages. It can be seen that the bare GCE gives a nearly straight line with an R_{et} of approximately 30 Ω (curve a). With the assembly of HANWA, the R_{et} of curve b increases to 527 Ω, reflecting that the modification of HANWA does not essentially affect the interfacial electron transfer in spite of HA's nonconductivity. That is, the densely distributed HANWA with large surface area and abundant adsorbing sites can provide a favorable electrochemical interface that would be facilitated for the construction of an electrochemical biosensor. This might be due to the inherent loose structure and multiadsorbing sites of the HA nanowires. The increase in interfacial transfer resistance was observed with an R_{et} of 2422 Ω (curve c) after HRP–CHIT immobilized onto the HANWA/GCE. The remarkable increment of electron transfer resistance indicates that the large surface area and particular multiadsorbing sites of HANWA facilitate the assembly of the HRP–CHIT layer.

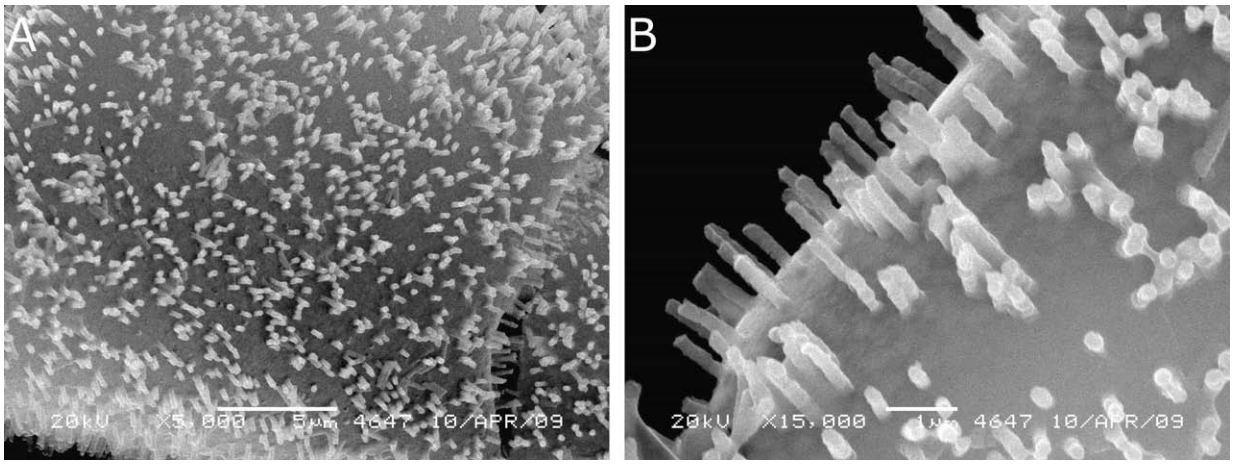

Fig. 1. Typical SEM images of the HANWA modified GCE: (A) low-magnification image; (B) high-magnification image. The electrodeposition was obtained under a constant cathode current of 0.005 mA mm^{-2} for 5 min.

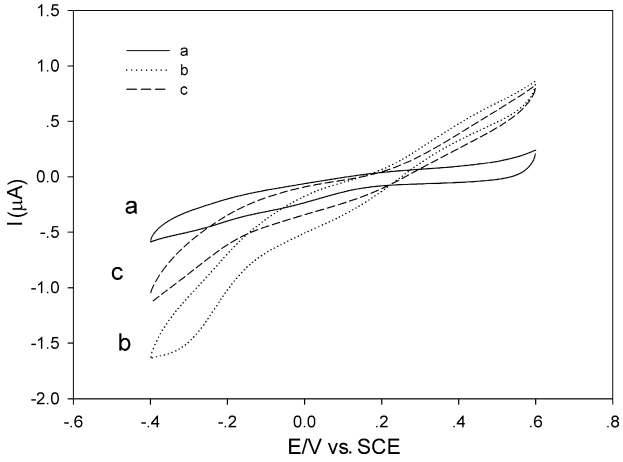

Fig. 3. CVs of the CHIT–HRP/HANWA biosensor in the following: (a) 10 mM PBS; (b) the same as curve a with 2 mM H_2O_2; (c) the same as curve b with 20 ng ml^{-1} cyanide standing 15 min before measurement for sufficient enzyme inhibition. Scan rate: 100 mV s^{-1}.

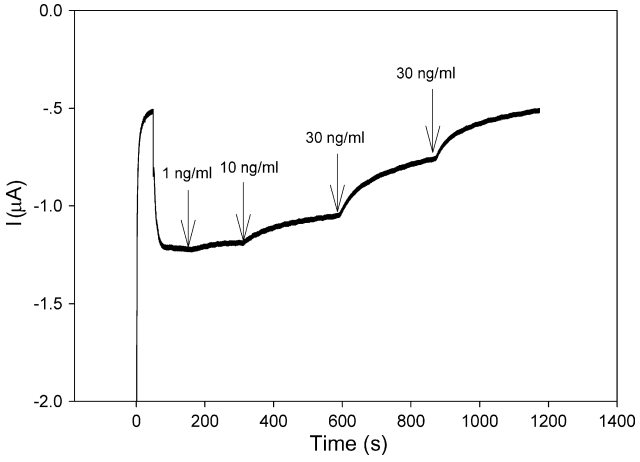

Fig. 4. Dynamic response of the CHIT–HRP/HANWA biosensor to 0.6 mM H_2O_2 and the successive addition of specific concentrations of cyanide in 10 mM PBS at a potential of −0.1 V.

The stability of the electrochemical interface was investigated by successive cyclic voltammograms (CVs) in PBS over a potential range from −0.4 to 0.6 V at a scan rate of 50 mV s^{-1}. The CHIT–HRP/HANWA/GCE biosensor is stable without significant current change during the consecutive 10 CV cycles (not shown).

HANWA with both overall positive and negative surface charges and particular multiadsorbing sites facilitates the spatially orientating adsorption and film-forming process. Due to well-aligned HANWA, the binding enzyme is not only abundant but also orderly in spatial orientation within the biofriendly environment. The CHIT's properties of excellent film-forming ability, good adhesion, biocompatibility, permeability, and high mechanical strength would also contribute to the performance of the designed biosensor. The current organic–inorganic hybrid nanostructure provides excellent enzyme–substrate contact with enzyme activity well maintained.

Enzyme inhibition by cyanide

To investigate the inhibition effect of cyanide on the immobilized HRP, CVs of the CHIT–HRP/HANWA/GCE biosensor were recorded in the specific solutions between −0.4 and 0.6 V at a scan rate of 100 mV s^{-1}, with the results shown in Fig. 3. When hydrogen peroxide was added, both the cathodic and anodic currents increased greatly due to the high specific catalysis of HRP (curve b). With the introduction of cyanide, the cathodic/reductive current decreased acutely (curve c), indicating the inhibition of HRP activity by cyanide.

Fig. 4 shows the dynamic responses of the CHIT–HRP/HANWA/GCE biosensor to 0.6 mM H_2O_2 and the successive addition of specific concentrations of cyanide in 10 mM PBS at a potential of −0.1 V. The start injection of hydrogen peroxide brings a distinct catalytic reduction current with a rapid steady state. Then the subsequent injections of specific concentrations of cyanide lead to the gradually decreasing reduction current. A slight current change can be observed with the addition of 1 ng ml^{-1} cyanide due to the inhibition of the enzyme. It can be seen from Fig. 4 that the inhibition signal increases with the increasing concentrations of cyanide. Because the concentration of H_2O_2 is certain, the reduction current depends only on the activity of enzyme. Therefore, the determination of cyanide can be realized according to the inhibition degree of cyanide on HRP.

HRP has a heme moiety as the active center to which the imidazole ring of the histidine residue is coordinated (fifth coordination site). The vacant sixth coordination site of the heme iron(III) is the reaction site for H_2O_2. Strong ligand of cyano group for heme impedes the approach of H_2O_2 to the active site; therefore, the H_2O_2 reduction current is depressed [26]. It allows Michaelis–Menten analysis of the electrocatalytic reduction of H_2O_2. In the absence of cyanide, the HRP electrode generates a constant current signal at a given peroxide concentration. When cyanide is introduced into the sample solution, it binds to the immobilized HRP, causing enzyme deactivation and, thus, reduced catalytic response. The apparent Michaelis–Menten constant (K_m^{app}) of the enzyme reaction at CHIT–HRP/HANWA/GCE can be calculated amperometrically according to the Lineweaver–Burk form [27] of the Michaelis–Menten equation:

$$\frac{1}{i_s} = \frac{K_m^{app}}{i_{max}} \times \left(\frac{1}{C}\right) + \frac{1}{i_{max}}.$$

Fig. 5 shows the Lineweaver–Burk plots of experimental results in the absence and presence of 10 ng ml^{-1} cyanide. The corresponding values of K_m^{app} and i_{max} derived from the linear plots for the uninhibited and inhibited enzymes of the biosensor were 4.90 mM and 721 nA (curve a) and 2.26 mM and 214 nA (curve b). The decrease in value of both K_m^{app} and i_{max} implies a more complicated inhibition mode that is different from the typical noncompetitive inhibition of

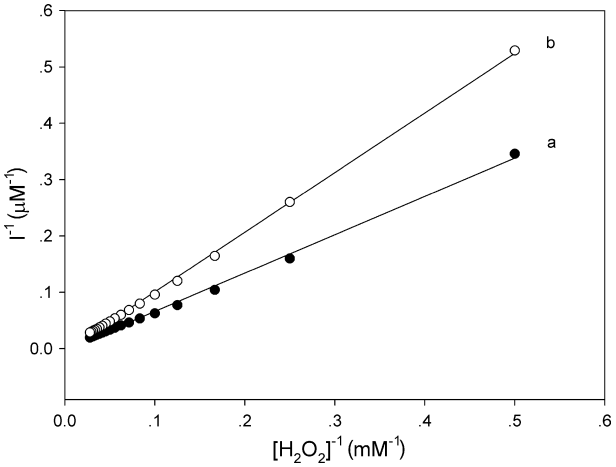

Fig. 5. Lineweaver–Burk plots of experimental results without cyanide (a) and with 10 ng ml^{-1} cyanide (b). Kinetic data were obtained by increasing levels of H_2O_2 in 2-mM increments under stirring.

the previous report [28]. It might be related to the characteristic of one-dimensional HANWA. Further work will be done on this subject.

Our experiments show that the cyanide inhibition on HRP can be recovered rapidly by rinsing thoroughly in ultrapure water right after the inhibition reaction, meaning the repetitious use of the as-prepared biosensor and suggesting a reversible inhibition of cyanide on HRP consistent with the previous report [27].

Cyanide inhibits the bioactivity of HRP with an effect of decreased reduction current. The percentage of inhibition was evaluated from the response of the active and inhibited forms of the enzyme. The immobilization procedure using aligned HANWA in the current study is biocompatible and spatial orientating; the enzyme molecules would effectively participate in the reaction. CHIT can entrap the enzyme with protection, allow substrate/inhibitor of fast diffusion, and provide resistance for outside interference to some degree. The HRP-bioencapsulated CHIT coating is permeable to small molecules and allows the detection of electrochemical active compounds that are present in the solution or generated during the biological recognition event.

Effect of applied potential

Fig. 6A shows the effect of the potential on the catalytic current to 2 mM H_2O_2. It can be seen that the catalytic current decreases with the increasing potential over the range of −0.2 to 0.15 V. When taking into account the inhibitory effect, the situation is not so simple. The degree of enzyme inhibition is a dynamic and relative process, so an investigation of potential on the percentage of inhibition was performed with the results shown in Fig. 6B. As can be seen in Fig. 6B, the inhibition degree (at two concentration levels of cyanide) is lower in more positive potentials, but the maximum value appears at −0.1 V. Therefore, the potential of −0.1 V was chosen in the current experiment.

Effect of pH

The influence of pH value is a more complex parameter related to enzyme activity, interface stability, and the existing form of cyanide that would directly affect the inhibition performance of the biosensor. Fig. 7 shows the inhibitory effect over the pH range from 4.9 to 9.2 in the presence of 16 ng ml^{-1} cyanide. The reasons for pH 7.65 achieving the best inhibitory effect are as follows: first, at this pH value, HRP retains good activity; second, HANWA and CHIT are stable in a weak alkaline environment; third, cyanide keeps an anion form in this case; and last, but very important, the pH value of 7.65 lies between the isoelectric point of HA (7.3) and that of HRP (8.3), which would promote the electrostatic constraint between HRP and HANWA. So, an ideal pH value of 7.65 could be recommended in this work.

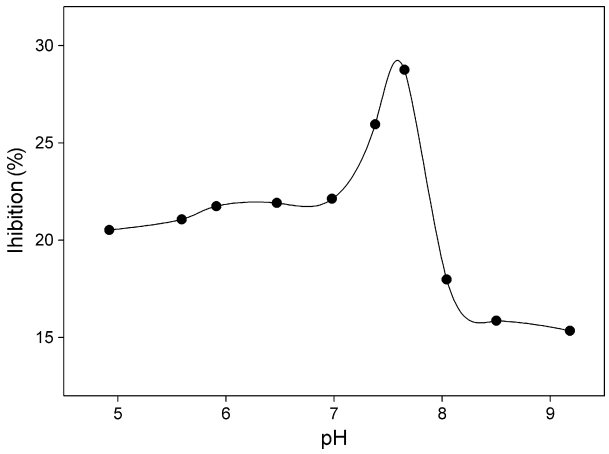

Fig. 7. Effect of pH on the percentage of inhibition to the addition of cyanide (16 ng ml^{-1}) in PBS containing 0.6 mM H_2O_2 at a potential of −0.1 V.

Effect of amount of H_2O_2

The changed amount of H_2O_2 would dynamically influence the inhibitory effect. In general, there is a trade-off between the sensitivity and the linear response range. A smaller amount of H_2O_2 will generate a smaller current signal by the enzyme electrode, and this will limit the linear range of the determination of cyanide. An increasing amount of H_2O_2 will give a wider response range with a sacrifice of sensitivity; however, too large an amount of H_2O_2 will cause most active centers of the enzyme to be occupied by the substrate and insensible to the inhibitor, and this would not meet the analytical requirement of cyanide detection. Fig. 8 shows the dependence of the amount of H_2O_2 on the percentage of inhibition to the addition of 8 ng ml^{-1} cyanide. The H_2O_2 concentration of 0.6 mM was chosen as a compromise for the assay.

Inhibition performance of cyanide biosensor

Chronoamperometry is a routine method for determining enzyme activity and inhibition. Here the decrease of the H_2O_2 reduc-

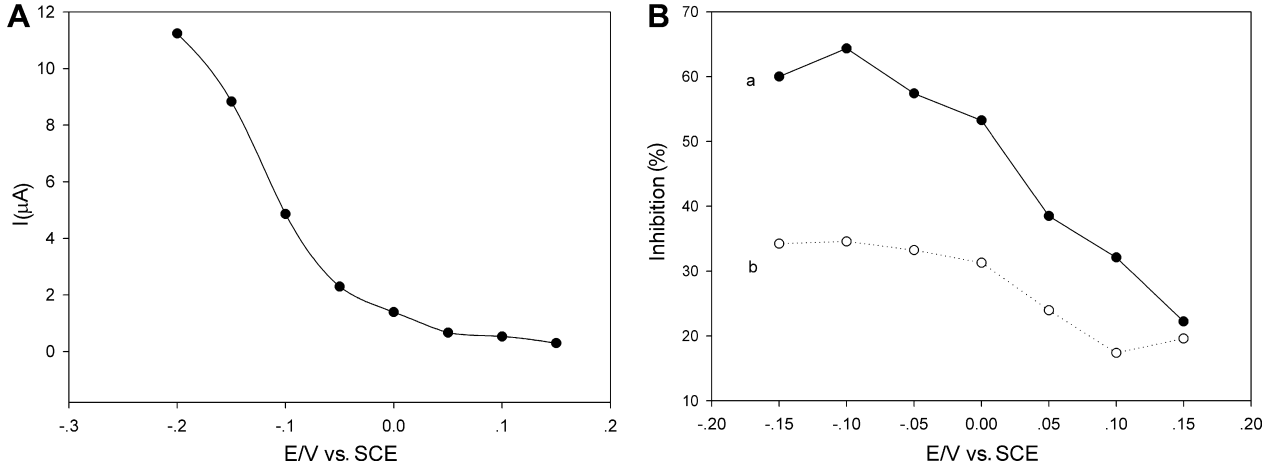

Fig. 6. Effect of potential on the reduction response of 2 mM H_2O_2 in PBS (A) and on the percentage of inhibition to the addition of cyanide at two concentration levels: 40 ng ml^{-1} (a) and 16 ng ml^{-1} (b) in PBS containing 0.6 mM H_2O_2 (B).

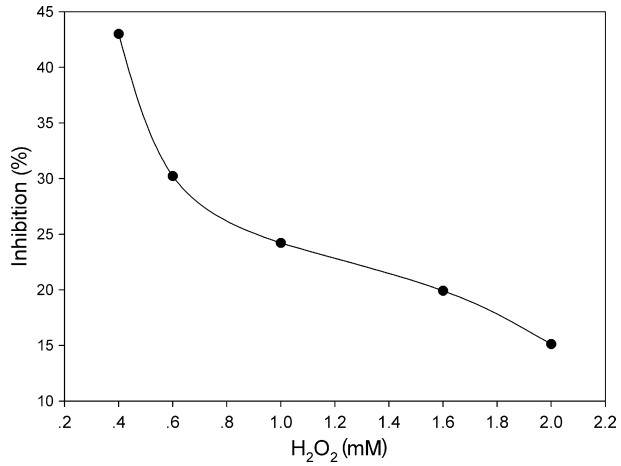

Fig. 8. Effect of amount of H_2O_2 on the percentage of inhibition to the addition of cyanide (8 ng ml^{-1}) in PBS at a potential of −0.1 V.

tion current serves as a measure of the cyanide concentration from the external sample solution. The quasi-steady-state current (within 10 min) is measured for each injection to construct the inhibition calibration curve. The inhibition percentage of the biosensor is calculated with the equation $I\,(\%) = [(I_0 - I_1)/I_0] \times 100$, where I_0 and I_1 are the quasi-steady-state currents of 0.6 mM H_2O_2 in 10 mM PBS (pH 7.65) without and with cyanide, respectively. Fig. 9 exhibits the calibration curve of cyanide under the optimized conditions in which the inhibition percentage of the biosensor is a function of cyanide concentration. The detection range of cyanide is 2–80 ng ml^{-1}, and the detection limit is 0.6 ng ml^{-1} obtained by 10% inhibition.

Selectivity is an important factor in the performance of an inhibition-based enzyme biosensor. Several cations and anions were measured to examine whether they interfered with the determination of cyanide. The effect of various possible interferences concurrently was investigated by the proposed biosensor for the determination of 10 ng ml^{-1} cyanide. From the results shown in Table 1, it can be seen that these ions will not interfere with the assay compared with the inhibition of cyanide except sulfide and cadmium. Further information on the dynamic profile of the inhibition process coupled with the powerful chemometrics method, as well as the response of the surface to different conditions, will be the subject of future research.

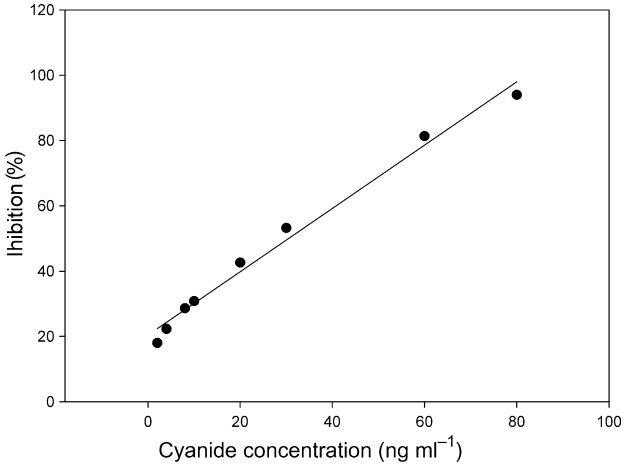

Fig. 9. Calibration curve of the percentage inhibition versus the concentration of cyanide under the optimized conditions.

Table 1
Data of interference experiments on analysis of 10 ng ml^{-1} cyanide by the proposed biosensor.

Test substance	Content[a]	Current ratio[b]
Cl^-	100	0.99
CO_3^{2-}	100	0.99
PO_4^{3-}	100	0.99
SO_4^{2-}	50	0.98
S^{2-}	5	0.65
Na^+	100	0.99
K^+	100	0.99
Hg^{2+}	10	0.97
Pb^{2+}	10	0.98
Cd^{2+}	10	0.82

[a] Ratio of content for interference to cyanide.
[b] Ratio of current for the mixtures to cyanide alone.

Table 2
Analysis of spiked tap water by the biosensor ($n = 3$).

Added (ng ml^{-1})	Found (ng ml^{-1})	Recovery (%)	RSD (%)
4.00	3.94	98.5	4.59
10.0	10.2	102.0	1.80
60.0	60.2	100.3	2.94

The reliability was checked by testing the spike samples (adding known amounts of cyanide to tap water), with the satisfactory recoveries presented in Table 2. To further demonstrate the applicability of the proposed biosensor, cyanide in river sample, distilled wine, and edible cassava starch was detected by the proposed biosensor and the calorimetric method. The obtained values were in good agreement by these two methods (Table 3).

The CHIT–HRP/HANWA/GCE biosensor can be recovered efficiently by a water rinse (~60 s) due to the reversible inhibition of cyanide on HRP. The regeneration is much more rapid than that of the related report [29], which was flushed overnight. Even after 30 cycle inhibition reactions, the biosensor can retain its original inhibition ability. The reproducibility of the proposed sensing system was investigated, and the relative standard deviations (RSDs) obtained for inter- and intra-assay of 20 ng ml^{-1} cyanide were 1.62% ($n = 6$) and 4.23% ($n = 6$), respectively. The operation life and shelf life of the cyanide biosensor were also investigated. The biosensor can retain an inhibition percentage close to the original within a single continuous use of 50 times. Long-term stability was studied by intermittent use of the storage biosensor, which was tested twice every day. When not in use, the biosensor was stored dry at 4 °C. The inhibition percentage to 10 ng ml^{-1} cyanide remained relatively constant for the first 20 days. Afterward, the response to H_2O_2 began to decrease and the inhibitory effect became unstable.

It should be mentioned that the detection limit of this proposed biosensor is lower than the detection limits of most reported cyanide sensors such as the optical sensor based on the immobilization of methyl violet [30] and porphyrin/myoglobin [31], the

Table 3
Determination of cyanide in real sample by the proposed biosensor and the calorimetric method (means ± SD, $n = 3$).

Sample	Content by the proposed biosensor (mg L^{-1} or mg kg^{-1})	Content by the calorimetric method (mg L^{-1} or mg kg^{-1})
River water	0.004 ± 0.001	0.005 ± 0.001
Distilled wine	0.086 ± 0.005	0.082 ± 0.001
Edible cassava starch	2.103 ± 0.016	2. 074 ± 0.011

piezoelectric quartz crystal microbalance sensor based on the selective chemical reaction between cyanide and the gold surface of the piezoelectric crystal [32], the light addressable photoelectrochemical sensor based on the *n*-CdSe electrode with the open circuit potential determined under illumination [33], the amperometric biosensor based on polyphenol oxidase and $Zn_3Al(OH)_8Cl$ clay [34] and HRP/[Zn-Cr-ABTS] redox clay [28] and based on asolectin, cytochrome *c*, and cytochrome oxidase modified carbon paste electrode that mimics a biological membrane environment [35], and the potentiometric biosensor based on immobilized cyanidase [36]. The low detection limit, short duration of time, economical use for reusability, and moderate linear range imply the successful design of the inhibition biosensor. In addition, the proposed cyanide biosensor was simple without coenzyme and extra mediator.

Conclusions

The current biosensor based on CHIT–HRP/HANWA allows not only high enzyme loading with native conformation but also easy electron transfer owing to the orderly spatial orientation, large surface area, and porosity. The immobilization of HRP is a hybrid style entrapping by CHIT on the nanoscale HANWA, which has strong adsorption with HRP and CHIT. The advantages of the developed cyanide biosensor, such as small sample size, sensitive detection, fast response, and rapid regeneration, make it an attractive alternative for the determination of pollutants in food or the environment and broaden the possible applications of chemosensors and biosensors.

Acknowledgments

This work was supported by the "973" National Basic Research Program of China (2007 CB 310500) and the National Natural Science Foundation of China (90817101 and 20775023).

References

[1] T.R. Kline, M. Tian, J. Wang, A. Sen, M.W.H. Chan, T.E. Mallouk, Template-grown metal nanowires, Inorg. Chem. 45 (2006) 7555–7565.
[2] R. Laocharoensuk, S. Sattayasamitsathit, J. Burdick, P. Kanatharana, P. Thavarungkul, J. Wang, Shape-tailored porous gold nanowires: from nano barbells to nano step-cones, ACS Nano 1 (2007) 403–408.
[3] R. Könenkamp, R.C. Word, M. Dosmailov, A. Nadarajah, Pentagonal ZnO nanorods, Phys. Stat. Sol. (RRL) 1 (2007) 101–103.
[4] A. Andreu, J.W. Merkert, L.A. Lecaros, B.L. Broglin, J.T. Brazell, M. El-Kouedi, Detection of DNA oligonucleotides on nanowire array electrodes using chronocoulometry, Sens. Actuat. B 114 (2006) 1116–1120.
[5] K. Ramanathan, M.A. Bangar, M. Yun, W. Chen, N.V. Myung, A. Mulchandani, Bioaffinity sensing using biologically functionalized conducting polymer nanowire, J. Am. Chem. Soc. 127 (2005) 496–497.
[6] K. Ohta, H. Monma, J. Tanaka, H. Eda, Interaction between hydroxyapatite and proteins by liquid chromatography using simulated body fluids as eluents, J. Mater. Sci. Mater. Med. 13 (2002) 633–637.
[7] R. Suena, S. Lina, W. Hsub, Hydroxyapatite-based immobilized metal affinity adsorbents for protein purification, J. Chromatogr. A 1048 (2004) 31–39.
[8] M. Niwa, W. Li, T. Sato, T. Daisaku, H. Aoki, H. Aoki, The adsorptive properties of hydroxyapatite to albumin, dextran, and lipids, Biomed. Mater. Eng. 9 (1999) 163–169.
[9] B. Wang, J.J. Zhang, Z.Y. Pan, X.Q. Tao, H.S. Wang, A novel hydrogen peroxide sensor based on the direct electron transfer of horseradish peroxidase immobilized on silica-hydroxyapatite hybrid film, Biosens. Bioelectron. 24 (2009) 1141–1145.
[10] Y. Li, X. Liu, X. Zeng, Y. Liu, X. Liu, W. Wei, S. Luo, Simultaneous determination of ultra-trace lead and cadmium at a hydroxyapatite-modified carbon ionic liquid electrode by square-wave stripping voltammetry, Sens. Actuat. B 139 (2009) 604–610.
[11] Y. Ding, J. Liu, H. Wang, G. Shen, R. Yu, A piezoelectric immunosensor for the detection of α-fetoprotein using an interface of gold/hydroxyapatite hybrid nanomaterial, Biomaterials 28 (2007) 2147–2154.
[12] S. Bose, S.K. Saha, Synthesis and characterization of hydroxyapatite nanopowders by emulsion technique, Chem. Mater. 15 (2003) 4464–4469.
[13] W.L. Meyer, Y. Liu, X.W. Shi, X.H. Yang, W.E. Bentley, G.F. Payne, Chitosan-coated wires: conferring electrical properties to chitosan fibers, Biomacromolecules 10 (2009) 858–864.
[14] Q. Sheng, K. Luo, J. Zheng, H. Zhang, Enzymatically induced formation of neodymium hexacyanoferrate nanoparticles on the glucose oxidase/chitosan modified glass carbon electrode for the detection of glucose, Biosens. Bioelectron. 24 (2008) 429–434.
[15] American Public Health Association, Method 4500-CN-E, in: L.S. Clescerl, A.E. Greenberg, A.D. Eaton (Eds.), Standard Methods for the Examination of Water and Wastewater, 20th ed., APHA, Washington, DC, 1998.
[16] E. Jungreis, F. Ain, Determination of cyanide in the p.p.b. range by atomic absorption spectrometry, Anal. Chim. Acta 88 (1977) 191–192.
[17] D.G. Themelis, P.D. Tzanavaras, Solvent extraction flow-injection manifold for the simultaneous spectrophotometric determination of free cyanide and thiocyanate ions based upon on-line masking of cyanides by formaldehyde, Anal. Chim. Acta 452 (2002) 295–302.
[18] A. Ishii, H. Seno, K. Watanabe-Suzuki, O. Suzuki, T. Kumazawa, Determination of cyanide in whole blood by capillary gas chromatography with cryogenic oven trapping, Anal. Chem. 70 (1998) 4873–4876.
[19] M. Nonomura, Indirect determination of cyanide compounds by ion chromatography with conductivity measurement, Anal. Chem. 59 (1987) 2073–2076.
[20] A.J. Curtis, C.C. Grayless, R. Fall, Simultaneous determination of cyanide and carbonyls in cyanogenic plants by gas chromatography–electron capture/photoionization detection, Analyst 127 (2002) 1446–1449.
[21] L.A. Terry, S.F. White, L.J. Tigwell, The application of biosensors to fresh produce and the wider food industry, J. Agric. Food Chem. 53 (2005) 1309–1316.
[22] S. Viswanathan, H. Radecka, J. Radecki, Electrochemical biosensor for pesticides based on acetylcholinesterase immobilized on polyaniline deposited on vertically assembled carbon nanotubes wrapped with ssDNA, Biosens. Bioelectron. 24 (2009) 2772–2777.
[23] D. Bagal-Kestwal, M.S. Karve, B. Kakade, V.K. Pillai, Invertase inhibition based electrochemical sensor for the detection of heavy metal ions in aqueous system: application of ultra-microelectrode to enhance sucrose biosensor's sensitivity, Biosens. Bioelectron. 24 (2008) 657–664.
[24] S. Manara, F. Paolucci, B. Palazzo, M. Marcaccio, E. Foresti, G. Tosi, S. Sabbatini, P. Sabatino, G. Altankov, N. Roveri, Electrochemically-assisted deposition of biomimetic hydroxyapatite–collagen coatings on titanium plate, Inorg. Chim. Acta 361 (2008) 1634–1645.
[25] M. Yang, F. Qu, Y. Lu, Y. He, G. Shen, R. Yu, Platinum nanowire nanoelectrode array for the fabrication of biosensors, Biomaterials 27 (2006) 5944–5950.
[26] R.A. Kamin, G.S. Wilson, Rotating ring-disk enzyme electrode for biocatalysis kinetic studies and characterization of the immobilized enzyme layer, Anal. Chem. 52 (1980) 1198–1205.
[27] T. Tatsuma, N. Oyama, H_2O_2-generating peroxidase electrodes as reagentless cyanide sensors, Anal. Chem. 68 (1996) 1612–1615.
[28] D. Shan, S. Cosnier, C. Mousty, Subnanomolar cyanide detection at polyphenol oxidase/clay biosensors, Biosens. Bioelectron. 20 (2004) 390–396.
[29] L. Su, J.B. Kelly, F.M. Hawkridge, M.C. Rhoten, S.I. Baskin, Characterization of cyanide binding to cytochrome *c* oxidase immobilized in electrode-supported lipid bilayer membranes, J. Electroanal. Chem. 581 (2005) 241–248.
[30] A. Afkhami, N. Sarlak, A novel cyanide sensing phase based on immobilization of methyl violet on a triacetylcellulose membrane, Sens. Actuat. B 122 (2007) 437–441.
[31] J.A. Legako, B.J. White, H.J. Harmon, Detection of cyanide using immobilized porphyrin and myoglobin surfaces, Sens. Actuat. B 91 (2003) 128–132.
[32] Y.G. Timofeyenko, J.J. Rosentreter, S. Mayo, Piezoelectric quartz crystal microbalance sensor for trace aqueous cyanide ion determination, Anal. Chem. 79 (2007) 251–255.
[33] S. Licht, N. Myung, Y. Sun, A light addressable photoelectrochemical cyanide sensor, Anal. Chem. 68 (1996) 954–959.
[34] D. Shan, C. Mousty, S. Cosnier, HRP/[Zn-Cr-ABTS] redox clay-based biosensor: design and optimization for cyanide detection, Anal. Chem. 76 (2004) 178–183.
[35] A. Amine, M. Alafandy, J.M. Kauffmann, Cyanide determination using an amperometric biosensor based on cytochrome oxidase inhibition, Anal. Chem. 67 (1995) 2822–2827.
[36] M. Keusgen, J.P. Kloock, D.T. Knobbe, M. Jünger, I. Krest, M. Goldbach, W. Klein, M.J. Schöning, Direct determination of cyanides by potentiometric biosensors, Sens. Actuat. B 103 (2004) 380–385.